LA-9210-MS

UC-5

Los Alamos National Laboratory is operated by the University of California for the United States Department of Energy under contract W-7405-ENG-36.

Response of Standard and High-Capacity HEPA Filters to Simulated Tornado and Explosive Transients

Los Alamos
Los Alamos National Laboratory
Los Alamos, New Mexico 87545

This work was supported by the US Department of Energy, Division of Waste Management.

LA-9210-M

UC-38
Issued: March 1982

Response of Standard and High-Capacity HEPA Filters to Simulated Tornado and Explosive Transients

W. S. Gregory
P. R. Smith*

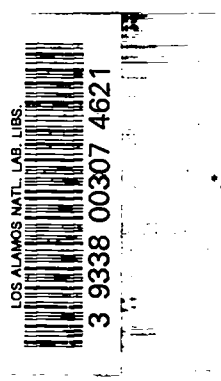

*Mechanical Engineering Department, New Mexico State University, Las Cruces, NM 88001

Los Alamos National Laboratory
Los Alamos, New Mexico 87545

RESPONSE OF STANDARD AND HIGH-CAPACITY HEPA FILTERS TO SIMULATED TORNADO AND EXPLOSIVE TRANSIENTS

by

W. S. Gregory and P. R. Smith

ABSTRACT

We have performed an investigation to determine the response of standard and high-capacity high-efficiency particulate air filters to simulated tornado and explosive transients. Most of the tests were directed toward evaluating the structural response of high-capacity filters to explosive transients. Selected tests were performed to evaluate the effects of particulate loading on filtration efficiencies. Also, we subjected several of the high-capacity filters to simulated tornado transients.

Our results indicate that the upper structural limits of high-capacity filters for explosive loading is 6.89-kPa (1-psi) peak pressure and 100-kPa-ms (14.51-psi-ms) impulse. These limits are below the approximately 13.78-kPa (2-psi) peak pressure loadings found for standard HEPA filters. Our tests of high-capacity filters preloaded with aerosol indicated that the structural limits were further degraded by approximately 40%. The filtration efficiencies were degraded to approximately 70% when the filters were subjected to aerosol entrained within the shock pulse. The effect of simulated tornado transients on high-capacity filters resulted in an upper structural limit of 11.02 kPa (1.6 psi) for peak pressure.

I. INTRODUCTION

Within nuclear facilities, pressure transient conditions might occur from man-caused accidents or natural phenomena. Man-caused accidents include gas explosions (for example, hydrogen), dust explosions, or chemical explosions. Natural phenomena such as tornadoes and their characteristic atmospheric

depressurization can also induce pressure surges. A knowledge of how the pressure transients from such events will affect the ventilation system of a nuclear facility is necessary to evaluate the probability of a release of radioactive particulate to the atmosphere. High-efficiency particulate air (HEPA) filters, common to nuclear facility ventilation systems, prevent radioactive particulates from being exhausted to the atmosphere at the facility boundaries under normal operating conditions. Typically, these filters have efficiencies of 99.97% or better. However, little is known about their efficiency or their structural response when they are struck by explosively driven shock waves or must respond to tornado-induced airflow. Therefore, the current study of shock and simulated tornado effects on the response of HEPA filters provides critical information for safety analysis of nuclear facilities.

Eight types of HEPA filters from six different manufacturers were tested. These included both standard and high-capacity filters made by both domestic and foreign manufacturers. However, the primary emphasis in this study was directed toward the response of high-capacity HEPA filters. Figure 1 shows a V-type HEPA filter made by the Luwa company in Switzerland. This filter has a rated airflow of .85 m^3/s (1800 cfm) compared with standard HEPA filter airflow rates of .47 m^3/s (1000 cfm). All of the high-capacity filters tested were of the V-type with the exception of a separatorless filter made by Flanders. The Department of Energy (DOE), Division of Airborne Waste Management, is interested in installing these types of filters in their facilities because their high airflow rates provide a longer life and a reduction in filter waste volume. Although these filters show promise for reducing radioactive waste, the DOE is also concerned with the response of these types of filters to abnormal operating conditions.

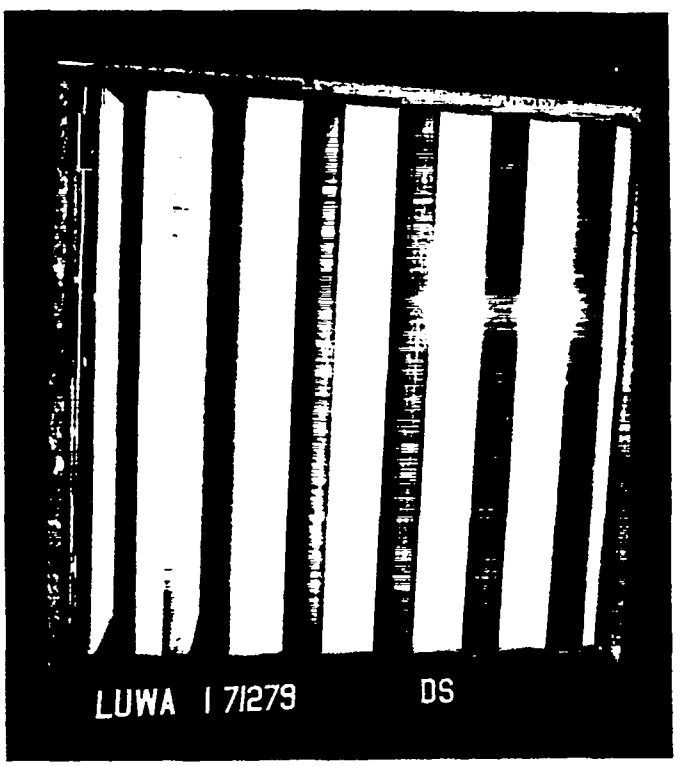

Fig. 1.
Typical high-capacity, V-type HEPA filter.

Sixty-three tests were made to determine both structural response and efficiency of these filters to a variety of dynamic over-pressures. Most of these tests were devoted to simulating explosive transients. However, we subjected a limited number of high-capacity filters to simulated tornado transients.

II. DESCRIPTION OF TEST APPARATUS

A. Tornado Transients Simulation

We reported simulation of tornado-induced pressure differentials across standard HEPA filters in Ref. 1. In the current tests, the same blowdown apparatus was used to subject the high-capacity filters to tornado pressure differentials. Additional details describing this apparatus are reported in Sec. III.A.

B. Explosive Transient Simulation

We simulated variable explosive waves using the Los Alamos National Laboratory/New Mexico State University (NMSU) shock tube. The apparatus is 0.91 m (36 in.) in diameter and has a variable-length driver section that is used to control both shock over-pressure and shock impulse. Thus, explosive shock waves can be simulated in terms of magnitude and distance from the source of the explosion.

Figure 2 is a photograph of the overall shock tube, which is located on the NMSU campus in Las Cruces, New Mexico. We have published reports about small-scale shock tube experiments and proposed experiments, shock-tube conceptual design, and construction details of the 0.91-m (36-in.)-diam shock tube.[2--4] The total length of the shock tube is approximately 48.77 m (160 ft). The tube consists of three sections, all made of 0.91-m (3-ft)-i.d. steel pipe. The sections are (1) a driver or high-pressure section that is 11.76 m (38 ft 7 in.) long, (2) an interstage or double-diaphragm section that is 0.43 m (17 in.) long, and (3) a driven or low-pressure section that is 36.58 m (120 ft) long. These sections appear from right to left, respectively, in Fig. 2.

The driver section can be pressurized to a maximum of about 2413.25 kPa (350 psig) by a large diesel-driven compressor. Therefore, peak pressure differences across the generated shock wave will be a maximum of approximately 344.75 kPa (50 psig). Dwell time of the pressure rise behind the shock wave can be varied from a few milliseconds to approximately 50 ms.

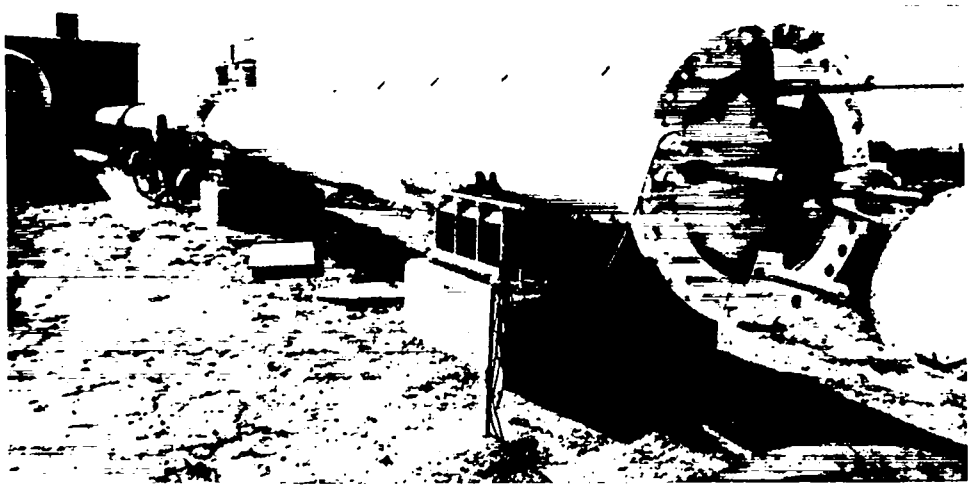

Fig. 2.
Photograph of the overall shock tube.

The dwell time of the pressure rise (and therefore the impulse) is controlled by varying the length of the driver (high-pressure) section, which is achieved through using a movable wall. The movable wall is sealed by a pneumatically expanded rubber tube around its rim. A system of movable steel carts (that is, load-carrying spacers) transfer the large axial forces (as high as 1 583 488 N or 356 000 lb) to the rear support flange and put the pipe in tension.

The shock tube is fired to generate its simulated explosive wave by rupturing metal or plastic diaphragms separating the driver section from the driven section. A short, 0.43-m (17-in.) length of 0.91-m (3-ft) tubing is placed between the driver section and the driven section. A thin diaphragm of a diameter equal to the flange diameters is placed on both ends of the interstage section. Both the interstage and driver sections are movable. After the diaphragms are in place, a pneumatic piston slides the driver forward until it clamps the interstage against the driven section. The final pressure seal is obtained by bolting the flanges of the sections together with 0.0508-m (2-in.)-diam bolts.

The firing sequence is as follows. (1) Pressurize the interstage region between the diaphragms to one-half the desired driver pressure. The diaphragm material has been selected so that it will not break at this differential

pressure. (2) Pressurize the driver section to a level to achieve the desired shock pressure. (3) Actuate a 0.0508-m (2-in.) solenoid valve that exhausts the interstage section to the atmosphere. The sudden drop in pressure in the interstage region causes the diaphragm between the driver and interstage sections to rupture. The subsequent large air impulse against the second diaphragm causes it to rupture sharply, and a shock wave then forms in the driven section and proceeds down the tube to the test section. The advantages of this firing method are that no mechanical devices are needed inside the tube to initiate firing, and the repeatability of initial pressures is assured for subsequent tests because premature rupture of diaphragms is eliminated.

C. Aerosol Preloading System

The aerosol preloading system used in these tests is the same system that has been described in Ref. 1. The aerosol used in the current study was polystyrene latex with an average particle diameter of 0.46μ.

III. METHOD OF TESTING

A. Tornado Transients

The method of testing standard HEPA filters is described in great detail in Ref. 1. The testing arrangement and procedure are based on maintaining a differential pressure across the test filter. We believe that this is equivalent to conditions that could exist as a tornado lowers the atmospheric pressure outside a nuclear facility. This concept is illustrated in Fig. 3.

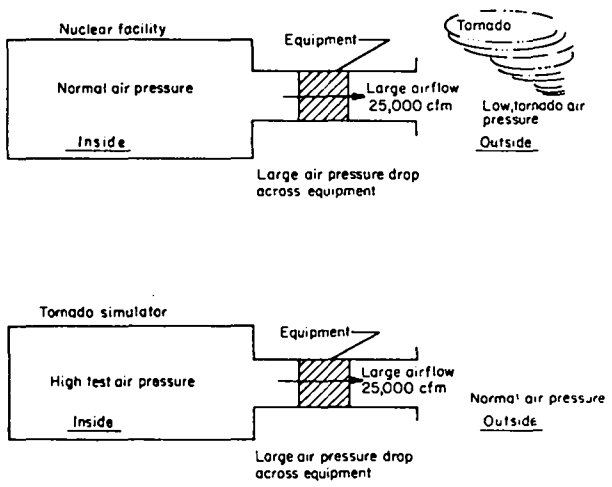

Fig. 3.
Comparison of actual tornado conditions and tornado simulator.

Differential pressure across the filter was measured by a Validyne model DP7 pressure transducer. A high-speed motion picture camera recorded the effects of the pressure pulse on the downstream face of the filter. Timing marks on the film were synchronized with timing marks on the pressure recording made on a Honeywell Visacorder. A schematic of this arrangement is shown in Fig. 4. The point of filter failure was found by examining the high-speed film and then finding the corresponding differential pressure on the chart recorder.

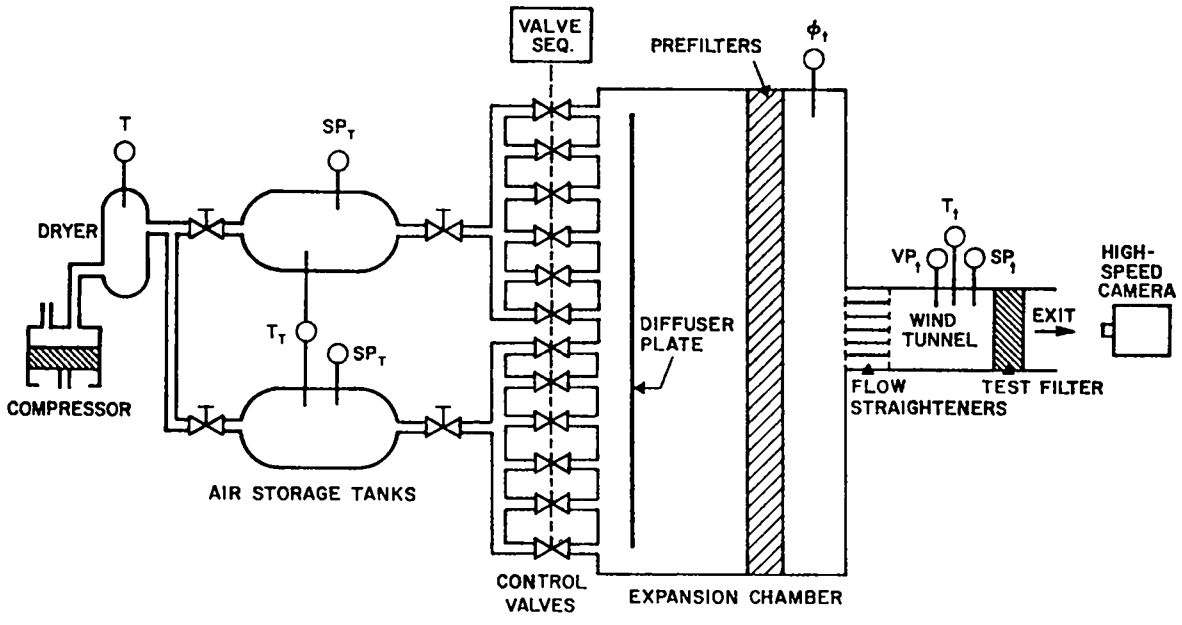

Fig. 4.
0.61-m by 0.61-m HEPA-filter tornado-model test-facility schematic.

B. Explosive Transients

Size 5 (0.61- by 0.61- by 0.30-m or 2- by 2- by 1-ft) HEPA filters were subjected to shock waves by placing them at the open end of the shock tube as shown in Fig. 5. A high-speed motion picture camera was placed downstream of the filter and focused on the face of the filter during the test (Fig. 6). A Kulite model XTH-1-190-10G pressure transducer with a frequency response of 10 000 Hz recorded the pressure of the passing shock wave 10 ft upstream of the filter. The value of the pressure was recorded on a Honeywell Visacorder (Model No. 2106). Timing marks on the high-speed film and the Visacorder were synchronized through a Redlake Corporation timing-light generator (Model No. 13-0001), thus allowing us to determine the time and pressure at the instant of filter failure. Several thermocouples in the driver and driven sections of the shock tube recorded static air temperatures before firing, which allowed us to determine wave velocities.

Testing proceeded by subjecting a single type of filter to progressively lower shock over-pressures (at a given driver length) until an over-pressure was reached for which the filter did not fail structurally. No filter was subjected to more than one test. Each filter was new and unused, and their costs ranged from $150 to $500. Therefore, to keep expenses down, most of the tests

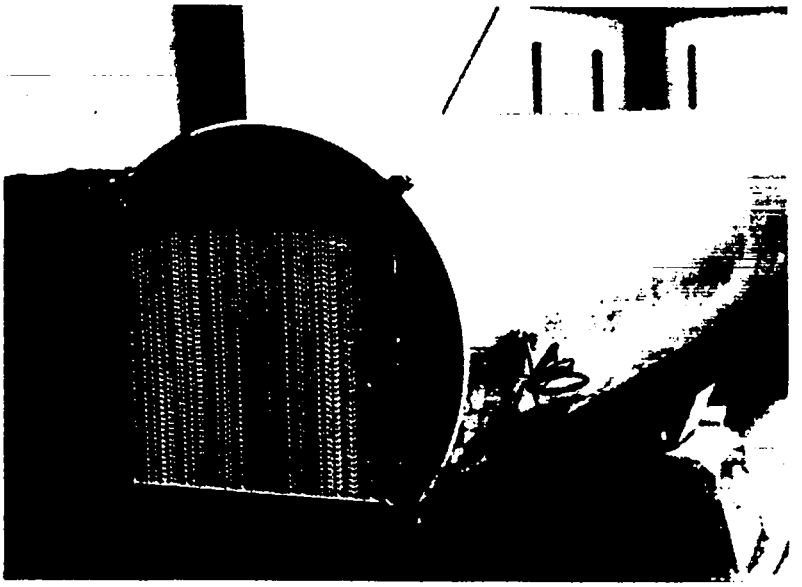

Fig. 5.
Size 5 HEPA filter ready for testing at exhaust end of the 36-in.-diam shock tube.

were conducted at a 9.75-m (32-ft) shock-tube driver length. Selected tests were then run for a 5.44-m (17.83-ft) and a 1.68-m (5.5-ft) driver length. After data reduction, we decided that four additional tests were necessary at the 5.44-m driver length.

C. Structural Testing of Preloaded Filters

We studied the effects of particulate loading on the structural response of HEPA filters exposed to shock waves. Several types of high-capacity filters

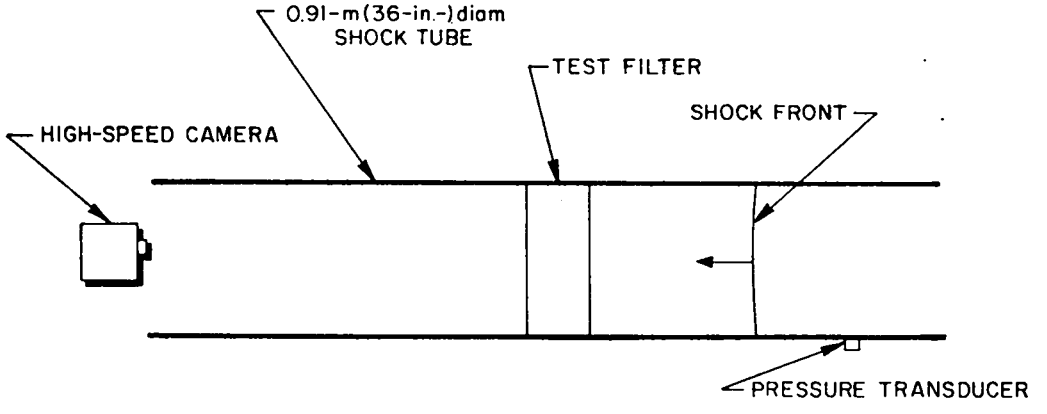

Fig. 6.
Schematic of HEPA filter shock testing apparatus and instrumentation.

were loaded with polystyrene latex particulate having a size range of 0.3 μ to 1.0 μ with a mean of 0.46 μ. Particulate generation was by a Laskin-type generator, and the particulate was entrained by an airflow of .85 m^3/s (1800 cfm), which then impinged upon the test filter.[1] Filters were loaded until a pressure drop of 38.1 cm (15 in.) was obtained. At this pressure drop, approximately 1 kg (.45 lb) of material had been deposited upon the filter.

The actual testing of the loaded filters for structural response to shock impingement proceeded identically to the tests of clean filters (see Sec. B). By using the results from the testing of the clean filters, fewer tests were required to obtain the structural failure limits of the loaded filters. All tests were conducted at a 5.44-m (17.83-ft) driver length.

D. Measurement of Mass Release From Loaded Filters

To determine the amount of mass that might be released from filters loaded with particulate upon impingement by a shock wave, filters were loaded as described in Sec. C. Five nucleopore filters were placed downstream of the filter on the end of the shock tube as shown in Fig. 7. Their exact placement is shown in Fig. 8. The face of each nucleopore filter was 5 cm (2 in.) from the downstream face of the high-capacity HEPA filters. A vacuum of 12 cm Hg applied to the rear of the nucleopore filters during the shock over-pressure assured that the released particulate would collect on the nucleopore filters.

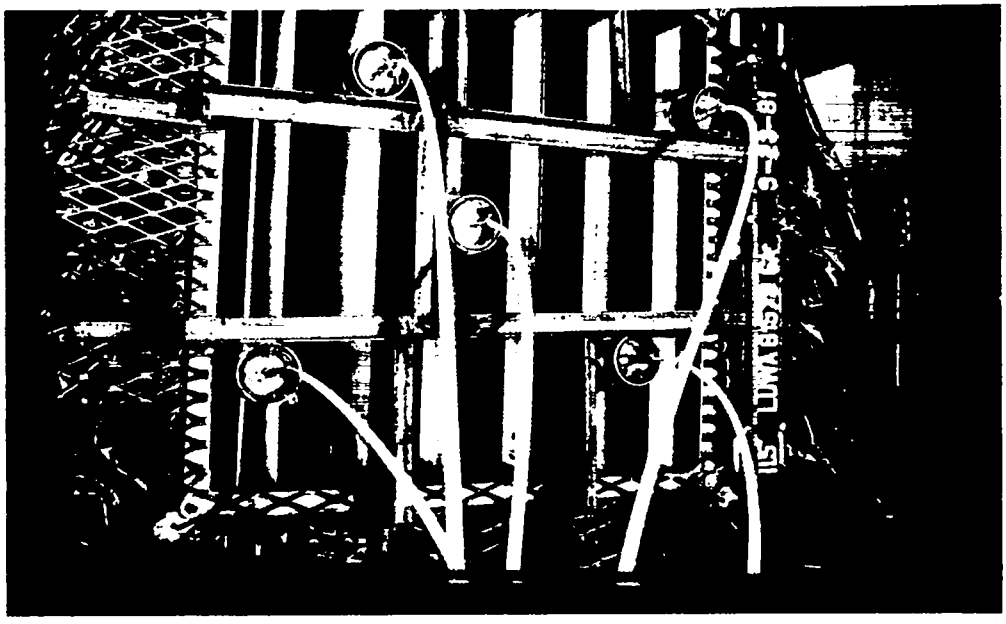

Fig. 7.
Photo of nucleopore filter holders on shock tube.

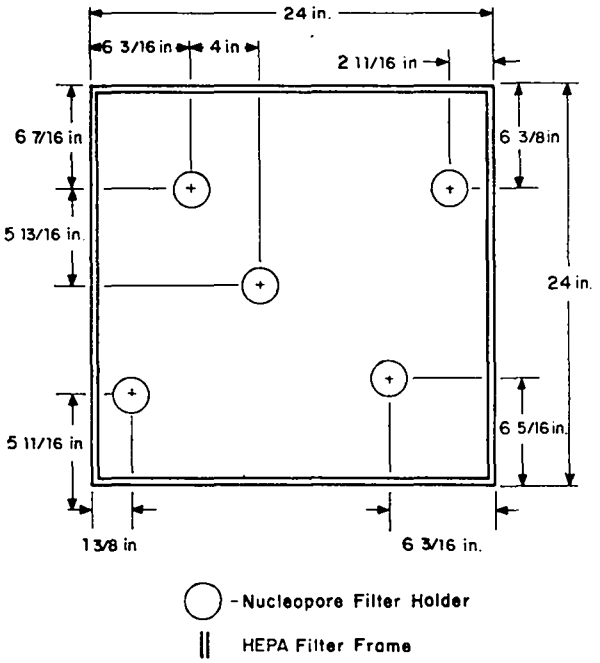

Fig. 8.
Schematic of nucleopore filter locations.

Each loaded filter was subjected to only one shock over-pressure. We selected shock over-pressures so that they were just below the structural failure limits found during the structural testing of loaded filters.

After a shock test, the nucleopore filters were examined with an electron microscope, and the number of particles released was determined by a direct count.

E. Filter Efficiency During Shock Over-Pressure

The efficiency of HEPA Filters during shock over-pressures was examined by first loading the driven section of the shock tube with a polystyrene latex aerosol from a Laskin generator. Five nucleopore filters were placed downstream of a clean high-capacity HEPA filter located at the exhaust of the shock tube (see Sec. D). Samples of the aerosol were analyzed by a Royco particle counter just before the shock tube was fired to determine the uniformity of distribution within the shock tube. If a satisfactory distribution existed, then the shock tube was fired; particulate was collected during the shock over-pressure by the nucleopore filters, which were again subjected to 12 cm Hg vacuum. Particulate counts for the nucleopore filters were determined using an electron microscope. Measuring the face velocity at the nucleopore filter and the known velocity of the air during the shock over-pressure allowed us to calculate the average efficiency of the HEPA filter during the shock pulse.

IV. RESULTS

A. Clean Filters Subjected to Simulated Tornado Transients

Table I lists the effects of the simulated tornado transients on high-capacity HEPA filters from four different manufacturers; the second and third columns contain the maximum differential pressure (ΔP_{max}) during the test and the differential break pressure (ΔP_{Brk}) for the filter. The fourth column lists the pressurization rate from time zero to the break (PR).

TABLE I

BREAK PRESSURES FOR TORNADO TESTS

Filter Mnf*	ΔP_{max} kpa	ΔP_{max} psi	P_{brk} kpa	P_{brk} psi	Pressurization Rate (PR) kpa/s	Pressurization Rate (PR) psi/s
AAF-V	22.74	3.3	6.89	1.0	12.40	1.8
AAF-V	21.36	3.1	10.34	1.5	10.34	1.5
FLN_S	13.09	1.9	11.02	1.6	16.54	2.4
FLN_S	11.02	1.6	11.02	1.6	13.09	1.9
FLN_S	11.71	1.7	11.02	1.6	13.78	2.0
Luwa	19.29	2.8	16.54	2.4	19.98	2.9
Luwa	20.67	3.0	15.85	2.3	19.29	2.8
Luwa	18.60	2.7	15.16	2.2	16.54	2.4
S.F.	17.23	2.5	9.65	1.4	8.96	1.3
S.F.	19.29	2.8	8.27	1.2	7.58	1.1

*Key to Manufacturer Code: FLN_S = Separatorless High-Capacity Flanders, Luwa = V-type High-Capacity Luwa, S. F. = V-type High-Capacity Sofiltra-Pulmen, AAF-V = V-type High Capacity American Air Filter.

B. Clean Filters Subjected to Simulated Explosive Transients

Table II is a summary of the test results. The first and second columns indicate the filter manufacturer and the sequence number of the test. The driver length (L_{DR}) appears in the third column, and the shock over-pressure (P_{max}) appears in the fourth column. The fifth column indicates whether the filter failed structurally during the tests (yes or no). The integral of the pressure over time ($\int pst$) up to the point of filter failure is listed in the sixth column and is equivalent to impulse per unit area. The time from the instant the shock wave strikes the filter until the filter fails (Δt) is in the last column. Notice that the tests are listed in order by filter manufacturer, driver length, and shock over-pressures. The typical damage to the downstream face of filters that were subjected to the explosive transients is shown in Fig. 9.

C. Preloaded Filters Subjected to Simulated Explosive Transients

Three of the four manufactured high-capacity filters were preloaded with polystyrene latex aerosol and then subjected to simulated explosive transients. Test results are shown in Table III. Structural and particulate release tests could not be made simultaneously. Therefore, those tests that were performed to determine structural effects are identified. As shown in Table III, all of

TABLE II

SUMMARY OF EXPERIMENTAL DATA

Filter Mnf*	Test No.	L_{DR} m	L_{DR} ft	P_{max} Kpa	P_{max} psi	Break?	$\frac{I}{A} = \int p\Delta t$ kpa-ms	$\frac{I}{A} = \int p\Delta t$ psi-ms	Δt ms
FLN	18	9.75	32	6.07	0.88	No	---	---	---
FLN	17	9.75	32	8.27	1.2	Yes	229.6	33.3	28
FLN	8	9.75	32	15.03	2.18	Yes	166.17	24.1	11
FLN	7	9.75	32	16.55	2.4	Yes	66.74	9.68	4
CAM	2	9.75	32	16.55	2.4	No	---	---	---
CAM	10	9.75	32	17.93	2.6	Yes	609.52	88.4	34
CAM	1	9.75	32	20.0	2.9	Yes	491.61	71.3	31
MSA	16	9.75	32	8.62	1.25	No	---	---	---
MSA	15	9.75	32	10.34	1.5	Yes	375.09	54.4	37
MSA	11	9.75	32	15.17	2.2	Yes	428.87	62.2	28
MSA	4	9.75	32	16.55	2.4	Yes	314.41	45.6	19
MSA	9	9.75	32	18.62	2.7	Yes	477.34	69.23	28
MSA	3	9.75	32	20.00	2.9	Yes	377.29	54.72	19
AAF	5	9.75	32	16.55	2.4	No	---	---	---
AAF	46	9.75	32	17.24	2.5	No	---	---	---
AAF	30	9.75	32	17.65	2.56	Yes	353.02	51.2	18
AAF	47	9.75	32	17.93	2.6	Yes	535.74	77.7	30
AAF	6	9.75	32	20.00	2.9	Yes	539.88	78.3	29
FLN_S	28	9.75	32	3.86	0.56	No	---	---	---
FLN_S	27	9.75	32	6.89	1.0	Yes	213.75	31	31
FLN_S	38	1.68	5.5	9.65	1.4	No	---	---	---
FLN_S	37	1.68	5.5	10.34	1.5	Yes	107.56	15.6	30
FLN_S	36	1.68	5.5	12.41	1.8	Yes	103.43	15	12
Luwa	19	9.75	32	7.58	1.1	No	---	---	---
Luwa	20	9.75	32	8.62	1.25	No	---	---	---
Luwa	48	9.75	32	9.86	1.43	Yes	345.44	50.1	35
Luwa	29	9.75	32	10.34	1.5	Yes		Film Lost	
Luwa	13	9.75	32	17.24	2.5	Yes		Film Lost	
Luwa	49	9.75	32	17.24	2.5	Yes	485.41	70.4	28
Luwa	12	9.75	32	19.31	2.8	Yes	405.43	58.8	21
Luwa	51	5.44	17.83	10.34	1.5	No	---	---	---
Luwa	50	5.44	17.83	12.41	1.8	Yes	335.10	48.6	27
Luwa	34	1.68	5.5	10.34	1.5	No	---	---	---
Luwa	35	1.68	5.5	12.07	1.75	No	---	---	---
Luwa	33	1.68	5.5	12.76	1.85	Yes	120.66	17.5	34

TABLE II CONT

SUMMARY OF EXPERIMENTAL DATA

Filter Mnf*	Test No.	L_{DR} m	L_{DR} ft	P_{max} Kpa	P_{max} psi	Break?	$\frac{I}{A} = \int p\Delta t$ kpa-ms	$\frac{I}{A} = \int p\Delta t$ psi-ms	Δt ms
Luwa	31	1.68	5.5	13.45	1.95	No	---	---	---
Luwa	32	1.68	5.5	14.82	2.15	Yes	136.52	19.8	212
S.F.	23	9.75	32	3.86	0.56	No	---	---	---
S.F.	22	9.75	32	6.89	1.0	Yes	262.01	38	38
S.F.	21	9.75	32	11.03	1.6	Yes	222.71	32.3	20
S.F.	14	9.75	32	15.86	2.3	Yes	222.02	32.2	14
S.F.	39	1.68	5.5	17.93	2.6	No	---	---	---
S.F.	40	1.68	5.5	19.31	2.8	No	---	---	---
S.F.	41	1.68	5.5	20.89	3.0	Yes	182.03	26.4	15
AAF-V	26	9.75	32	3.65	0.53	No	---	---	---
AAF-V	45	9.75	32	4.83	0.7	No	---	---	---
AAF-V	25	9.75	32	6.89	1.0	Yes	206.85	30	30
AAF-V	24	9.75	32	10.76	1.56	Yes	333.72	48.4	31
AAF-V	42	1.68	5.5	24.82	3.6	No	---	---	---
AAF-V	43	1.68	5.5	25.51	3.7	Yes	151.00	21.9	7

*Key to Manufacturer Code: FLN = Standard Flanders, CAM = Standard Cambridge, MSA = Standard Mine Safety Applicance, AAF= Standard American Air Filter, FLN_S = Separatorless High-Capacity Flanders, Luwa = V-type High-Capacity Luwa, S.F. = V-type High-Capacity Sofiltra-Pulmen, AAF-V = V-type High Capacity American Air Filter.

TABLE III

PRELOADED HIGH-CAPACITY HEPA FILTERS SUBJECTED TO SIMULATED EXPLOSIVE TRANSIENTS

Filter Mnf	Test No.	L_{DR} m	L_{DR} ft	P_{max} kPa	P_{max} psi	Break	$\frac{I}{t} = \int p\Delta t$ kPa-ms	$\frac{I}{t} = \int p\Delta t$ psi-ms	Δt ms	Particulate ms	Particles Released
Luwa	56	5.44	17.83	6.83	0.99	Yes	-	-	-	Yes	6.39×10^{15}
Luwa	58	5.44	17.83	6.48	0.94	Yes	-	-	-	No	*
Luwa	59	5.44	17.83	3.79	0.55	No	-	-	-	Yes	1.9×10^{10}
AAF-V	60	5.44	17.83	10.27	1.49	Yes	154.1	22.35	15	No	*
FLN_S	61	5.44	17.83	5.10	0.74	No	-	-	-	No	*
FLN_S	62	5.44	17.83	3.86	0.56	No	-	-	-	Yes	4.22×10^{10}
FLN_S	63	5.44	17.83	6.83	0.99	Yes	75.1	10.89	11	No	*

*Structural Test Only
-Not Measured

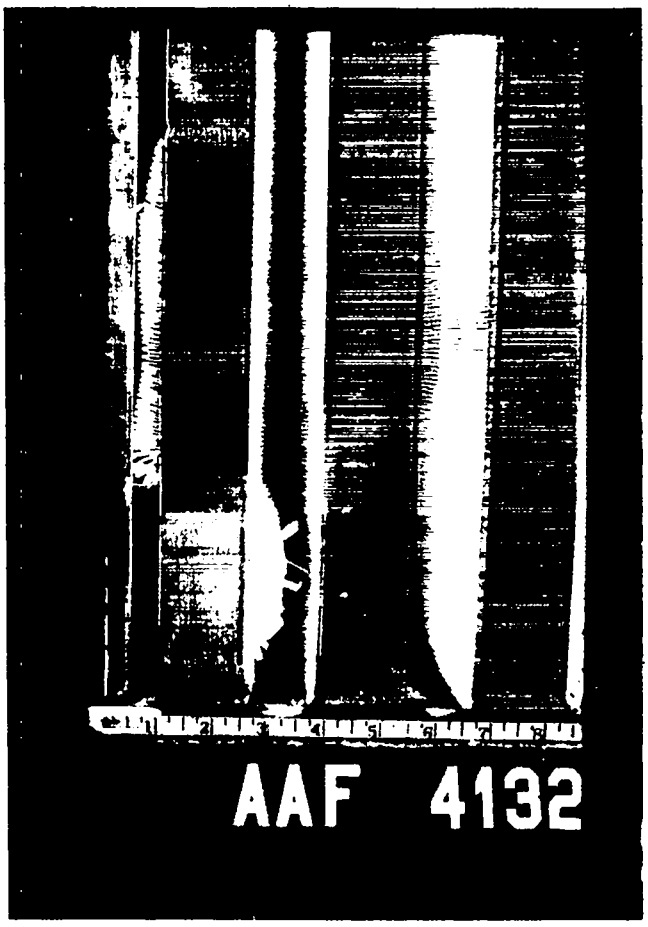

Fig. 9.
Downstream face of high-capacity HEPA filters subjected to explosive transients.

the tests were performed at an intermediate shock-tube driver length of 5.44 m (17.83 ft). The shock wave peak pressure is listed, as is a column indicating whether the filter failed.

Particle release measurements were made in three tests. The procedure used in making these measurements is discussed in Sec. III-D. Because of the limited number of tests and the method of measurement, the results are of a qualitative nature and should be used carefully. Figures 10 and 11 are electron microscope photographs of portions of the nucleopore filters for tests 56 and 59.

D. Efficiency of Clean Filters Subjected to Particulate Entrained Within Shock Pulse

Test number 57 was performed using a clean Luwa filter at a shock tube driver length of 5.44 m (17.83 ft). It did not break when subjected to a shock peak pressure of 6.89 kPa (1.0 psi). We made a particulate measurement upstream of the filter before testing using the Royco particle counter. The particle number that challenged the filter during the shock pulse was 4.59×10^{10}. The number of particles passing through the filter was 1.32×10^{10}.

Figure 12 is an electron microscope photograph of a portion of the center nucleopore filter downstream of the filter.

V. DATA ANALYSIS

A. Clean Filters Subjected to Simulated Tornado Transients

The break pressures for the high-capacity filters are listed in Table I. This information can be consolidated into the form shown in Table IV. Table IV

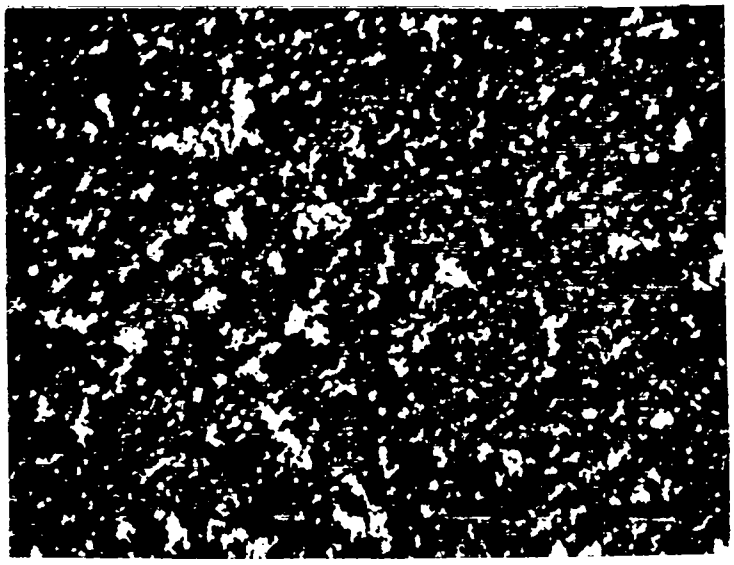

Fig. 10.
Electron microscope photo of test 56.

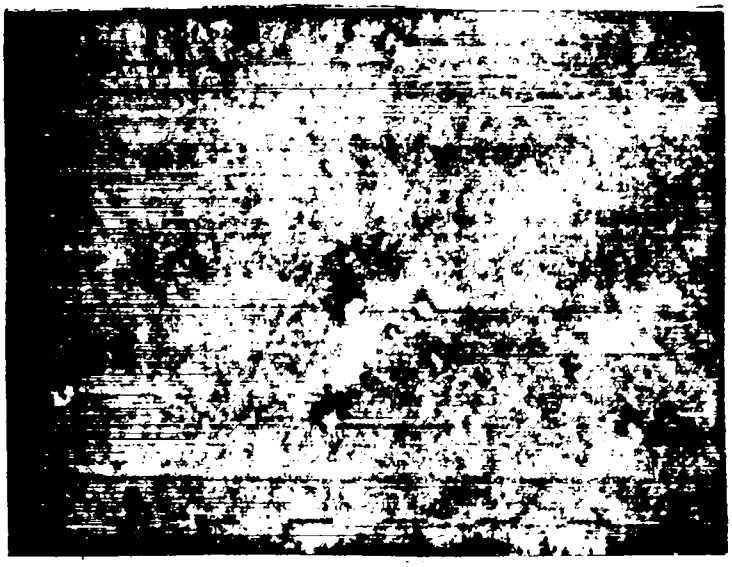

Fig. 11.
Electron microscope photo of test 59.

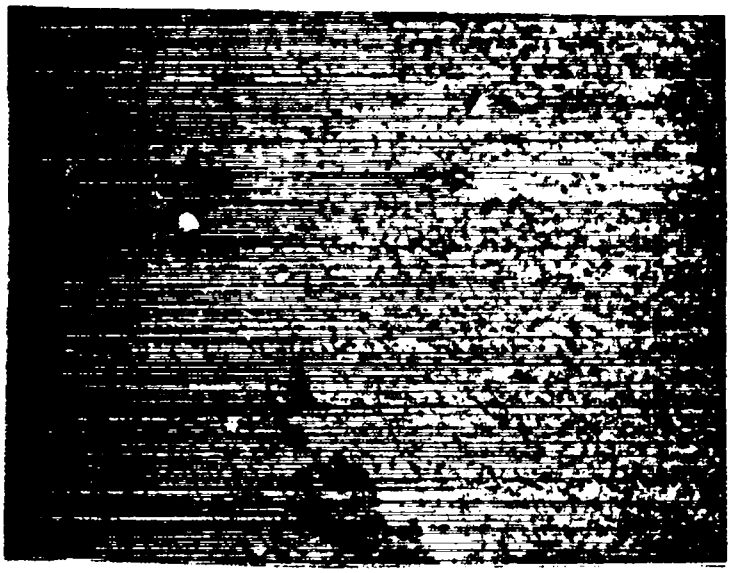

Fig. 12.
Electron microscope photo of test 57.

shows that the lowest break pressure for this type of filter is 9.0 kPa (1.3 psi), and the highest break pressure is 15.9 kPa (2.3 psi) and the average structural limit is 11.0 kPa (1.6 psi). This average value compares with a value of 16.4 kPa (2.4 psi) found for standard HEPA filters.[5] Thus, high-capacity HEPA filters are weaker than standard HEPA filters when they are subjected to similar simulated tornado loadings.

B. Clean Filters Subjected to Simulated Explosive Transients

The method we used to determine the shock over-pressures needed to cause a filter to fail is summarized in Table V. Again, the first column lists the filter manufacturer, the second column lists the test number, the third column lists the driver length, the fourth column shows the shock over-pressure, and the fifth column indicates whether failure occurred. Notice that two tests are listed for each type of filter and each driver length, one for which no failure occurred and one for which

TABLE IV

HIGH-CAPACITY HEPA FILTER BREAK PRESSURES FOR SIMULATED TORNADO TRANSIENTS

Filter Mnf	Filter Break Pressure kPa	psi
AAF-V	11.0	1.6
FLN_S	9.0	1.3
Luwa	15.9	2.3
S.F.	9.0	1.3
Average	11.2	1.6

TABLE V

SHOCK OVER-PRESSURE TO BREAK HIGH-CAPACITY
AND STANDARD HEPA FILTERS

Filter Mnf*	Test No.	L_{DR} m	L_{DR} ft	P_{max} kPa	P_{max} psi	Break?	P_{BRK} kPa psi	$\frac{I}{A} = \int p\Delta t$ kPa-ms	$\frac{I}{A} = \int p\Delta t$ psi-ms
FLN	18	9.75	32.0	6.07	0.88	No	7.17 ± 1.10		
FLN	17	9.75	32.0	8.27	1.2	Yes	(1.04 ± 0.16)	229.60	33.3
CAM	2	9.75	32.0	16.55	2.4	No	17.24 ± 0.69		
CAM	10	9.75	32.0	17.93	2.6	Yes	(2.5 ± 0.1)	609.52	88.4
MSA	16	9.75	32.0	8.62	1.25	No	9.52 ± 0.90		
MSA	15	9.75	32.0	10.34	1.5	Yes	(1.38 ± 0.13)	375.09	54.4
AAF	46	9.75	32.0	17.24	2.5	No	17.44 ± 0.21		
AAF	47	9.75	32.0	17.65	2.56	Yes	(2.53 ± 0.03)	535.79	77.7
FLN_S	28	9.75	32.0	3.86	0.56	No	5.38 ± 1.52		
FLN_S	27	9.75	32.0	6.89	1.0	Yes	(0.78 ± 0.22)	213.75	31.0
FLN_S	38	1.68	5.5	9.65	1.4	No	10.0 ± 0.34		
FLN_S	37	1.68	5.5	10.34	1.5	Yes	(1.45 ± 0.05)	107.56	15.6
Luwa	20	9.75	32.0	8.62	1.25	No	9.24 ± 0.62		
Luwa	32	9.75	32.0	9.86	1.43	Yes	(1.34 ± 0.09)	345.44	50.1
Luwa	51	5.44	17.83	10.34	1.5	No	11.38 ± 1.03		
Luwa	50	5.44	17.83	12.41	1.8	Yes	(1.65 ± 0.15)	335.1	48.6
Luwa	35	1.68	5.5	12.07	1.75	No	12.41 ± 0.34		
Luwa	33	1.68	5.5	12.76	1.85	Yes	(1.8 ± 0.05)	120.66	17.5
S.F.	23	9.75	32.0	3.86	0.56	No	5.38 ± 1.52		
S.F.	22	9.75	32.0	6.89	1.0	Yes	(0.78 ± 0.22)	262.01	38.0
S.F.	40	1.68	5.5	19.31	2.8	No	20.0 ± 0.69		
S.F.	41	1.68	5.5	20.69	3.0	Yes	(2.9 ± 0.1)	192.37	27.9
AAF-V	45	9.75	32.0	4.83	0.7	No	5.86 ± 1.03		
AAF-V	25	9.75	32.0	6.89	1.0	Yes	(0.85 ± 0.15)	206.85	30.0
AAF-V	42	1.68	5.5	24.82	3.6	No	25.17 ± 0.34		
AAF-V	43	1.68	5.5	25.51	3.7	Yes	(3.65 ± 0.05)	151.0	21.9

failure barely occurred. The shock over-pressure needed to fail the filter (P_{Brk}) was assumed to be the average of the shock over-pressure of these two tests. The uncertainty in P_{Brk} is taken to be one-half the difference between the shock over-pressures of the two tests. The remaining column of Table V gives the impulse per unit area ($\int p\Delta t$) up to the point of filter failure on the second tests.

Hence, from Table V we find that a standard Flanders filter (FLN) will fail at a shock over-pressure of 7.17 $\pm$ 1.10 kPa (1.04 $\pm$ 0.16 psi), and a Flanders separatorless filter (FLN_s) will fail at 5.38 $\pm$ 1.52 kPa (0.78 $\pm$ 0.22 psi) (both at 9.75-m (32-ft) driver lengths). However, we find that a FLN_s filter will fail at a shock over-pressure of 10.0 $\pm$ 0.34 kPa (1.45 $\pm$ 0.05 psi) if the driver length is 1.68 m (5.5 ft). We see from Table V that the shock over-pressure for which failure occurs increases with decreasing driver length for all filters tested. This item is summarized in Fig. 13 in which P_{BRK} is plotted as a function of driver length (L_{DR}).

The failure over-pressures found in these current tests for 9.75-m (32-ft) driver lengths (47 ms dwell) are all lower than those reported in the literature for similar testing. Anderson and Anderson[6] found that 0.61- by 0.61- by 0.3-m (24- by 24- by 12-in.) HEPA filters failed at over-pressures of about 21.96 $\pm$ 0.45 kPa (3.185 $\pm$ 0.065 psi). The dwell time behind their shock waves was approximately 50 ms. The manufacturers of the filters used in their tests were not revealed. The results of the current study certainly show that the breaking point of the filters subjected to shock over-pressure is dependent on the manufacturers. We tested the standard HEPA filters to establish a base-line comparison with the tests performed earlier by Anderson and Anderson.[6] Our results for structural strength of standard HEPA

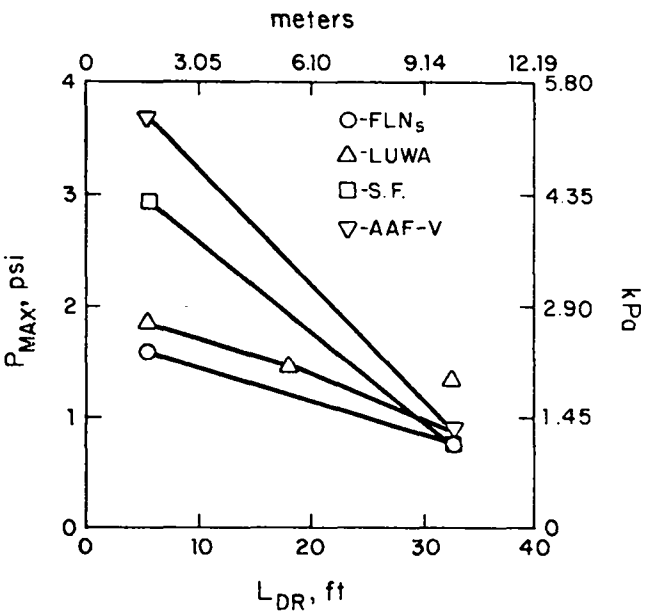

Fig. 13.
Shock over-pressure needed to just break high-capacity HEPA filters.

filters yield a lower average value than reported by Anderson and Anderson[6] (12.8 kPa or 1.86 psi) and are summarized in Table VI.

As the driver length is decreased, the time of dwell of the shock over-pressure decreases. Compare Fig. 14 with Fig. 15. Fig. 14 is a trace of the pressure for a long (9.75-m or 32-ft) driver section, and the latter is a trace of the pressure for a short (1.68-m or 5.5-ft) driver section. The dwell behind the shock wave is about 47 ms in the long driver case and about 5 ms in the short driver case. Our previous studies have shown that the reflected wave from the rim of the filter case that appears at the pressure transducer location about 20 ms after shock passage is not experienced on the face of the filter or interior to the filter.[7] The results (summarized in Fig. 13) appear to be justified because less impulse per unit area (that is, the integrated area under the pressure pulses shown in Figs. 14 and 15) is available at short driver lengths compared with long driver lengths for the same peak pressure. However, this logic presupposes that impulse causes filter failure. To examine this supposition, we consider Fig. 16, a plot of the impulse per unit area $I/A = \int p \Delta t$ as a function of driver length (L_{DR}), taken from Table V. If the impulse resulting from the shock over-pressure is the cause of failure, then the lines in Fig. 16 should be horizontal; that is, impulse should not be a function of driver length. Obviously, this is not true.

Careful examination of the pressure records reveals that for all the 1.68-m (5.5-ft)-long driver tests, filter failure occurred after the shock impulse had passed through (or more probably, had been absorbed by) the filter. In fact, in one case (Luwa α32) failure did not occur until 212 ms after the shock struck the filter. However, for the remainder of the cases, the failure occurred within 7 to 34 ms after shock impingement. This would seem to imply that some other mechanism contributes to the failure of the filter at the short (1.68-m or 5.5-ft) driver length. The cause of this phenomenon could be airflow rate. The passage of the shock wave through the air of the tube causes the air to move in the

TABLE VI

BREAK PRESSURES OF STANDARD HEPA FILTERS SUBJECTED TO SIMULATED EXPLOSIVE TRANSIENTS

Filter Mnf	Shock Wave Duration ms	Shock Overpressure to Break Filter kPa	psi
CAM	47	17.2	2.50
AAF	47	17.4	2.53
FLN	47	7.2	1.04
MSA	47	9.5	1.38
	Average	12.8	1.86

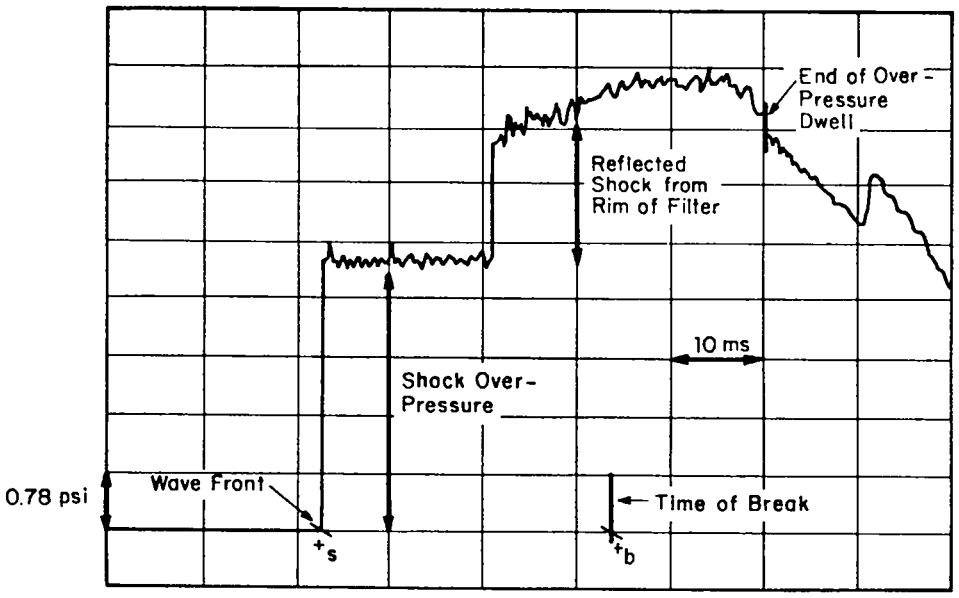

Fig. 14.
Typical pressure trace of shock over-pressure for a 32-ft driver length (pressure transducer located 10 ft upstream of filter).

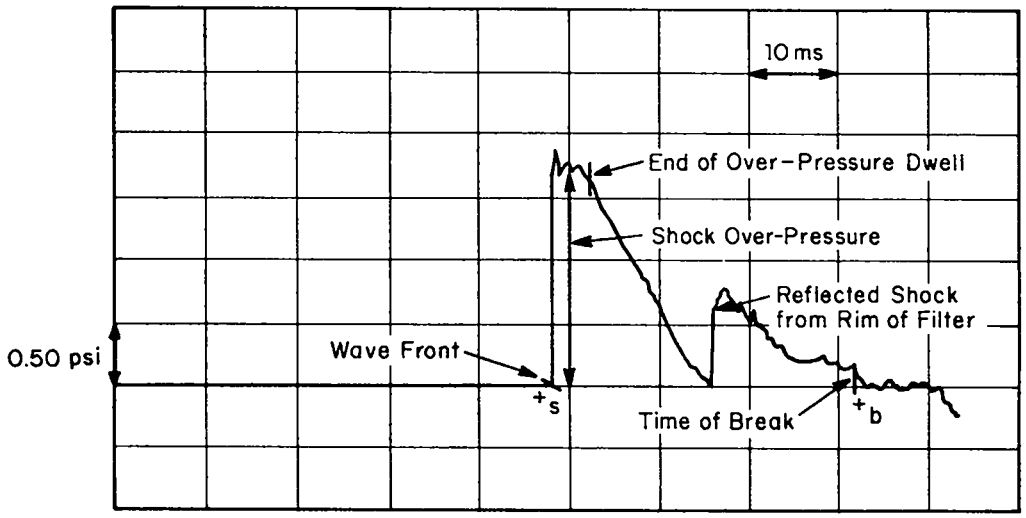

Fig. 15.
Typical pressure trace of shock over-pressure for a 5.5-ft driver length (pressure transducer located 10 ft upstream of filter).

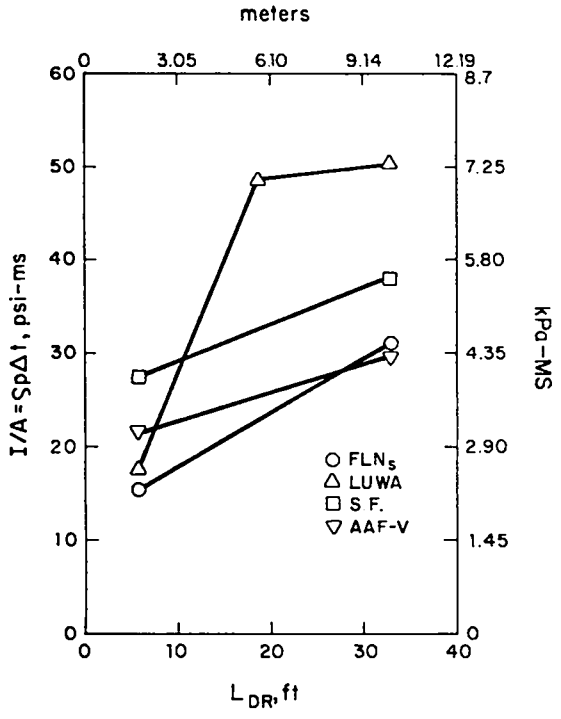

Fig. 16.
Shock impulse needed to just break HEPA filters.

same direction as the shock wave. The trailing expansion wave does not change the direction of this air movement.[8]

Notice from Fig. 13 that the lowest P_{Brk} at a 1.68-m (5.5-ft) driver length was 10 kPa (1.45 psi) for the FLN_S filter. The air velocity behind a shock wave with this over-pressure is 28.77 m/s (94.39 ft/s) or a flow rate through the filter of 10.69 m^3/s (22 654 cfm). For the S.F. filter, P_{Brk} at a 1.68-m (5.5-ft) driver length was 20.0 kPa (2.9 psi). The air velocity behind the shock wave with this over-pressure would be 52.15 m/s (171.1 ft/s) or a flow rate through the filter of 19.38 m^3/s (41 058 cfm). Our tornado testing of these filters showed that the flow rates through the filters reached a maximum value of 10.38 m^3/s (22 000 cfm) and that most filter failures occurred at flow rates below this value. Thus, because high residual airflow rates still persist after the passage of the shock impulse, it is probably this high flow rate, with its attendant high stagnation pressure, that causes the failure of the filters.

The odd point on the Luwa curve in Fig. 16 can now be explained. The value of I/A at L_{DR} = 5.44 m (17.83 ft) is the same as the value of I/A at L_{DR} = 9.75 m (32 ft) within the limits of error of the measurement $\pm$ 37 kPa ms ($\pm$ 5.4 psi-ms);* that is, for long driver lengths, it appears that the impulse needed to cause a filter to fail is constant for this type of filter. However, it would be dangerous to generalize this statement to all types of HEPA filters from the small number of data available for the Luwa filters.

---

*Appendix A contains the expected error of the experimental results in SI units. Appendix B contains the expected error of the experimental results in English units.

Therefore, we ran four more tests, one each for the FLN_s, Luwa, S.F. and AAF-V. All were at a driver length of 5.44 m (17.83 ft). The shock over-pressures were selected from Fig. 13, and we assumed a linear variation to the over-pressure just needed to break the filters with driver length. Table VII summarizes the results of these runs.

If the data of Tables V and VII are used to construct another plot of impulse per unit area ($I/A = \int p\Delta t$) as a function of driver length (L_{DR}), then Fig. 17 results. Notice that for filters FLN_s, Luwa, and S.F., I/A is essentially the same for driver lengths 5.44 m and 9.75 m (17.83 ft and 32 ft), which supports our hypothesis that, for long driver lengths, the shock impulse needed to just cause filter failure is constant for a particular type of filter. However, the AAF-V filter does not appear to support this statement. Examining the expected error bands in Appendix A, we found that for test AAF-V #54, the value of I/A is 179.88 kPa-ms with an error band of approximately $\pm$ 82.42 kPa-ms. The value of I/A at driver length 9.75 m (32 ft) for AAF-V #25 is 206.85 kPa-ms with an expected error of approximately $\pm$ 23.49 kPa-ms. Thus, within the limits of accuracy of the experiments, AAF-V #54 and AAF-V #25 give the same results for I/A. Therefore, there is a strong probability that the shock impulse needed to fail a particular type of filter is constant at long driver lengths. These results were reported at the 52nd Shock and Vibration Symposium, which was held on October 27--29, 1981.

C. Material Release from Preloaded High-Capacity Filters

The particulate released from loaded HEPA filters is given in Table III. Test number 56 was of a Luwa V-type high-capacity filter. The shock over-pressure for this test was 6.83 kPa (0.99 psi), and it caused the filter to fail slightly. Failure consisted of barely visible folds in the filter paper.

TABLE VII

SUPPLEMENTARY TEST DATA

Filter Mnf.	Test No.	L_{DR} m	L_{DR} ft	P_{max} kPa	P_{max} psi	Break?	$\frac{I}{A} = \int p\Delta t$ kPa/ms	$\frac{I}{A} = \int p\Delta t$ psi-ms	Δt ms
FLN_s	55	5.44	17.83	8.89	1.29	Yes	204.84	29.71	23
Luwa	52	5.44	17.83	11.59	1.68	Yes	359.63	52.16	31
S.F.	53	5.44	17.83	13.46	1.95	Yes	269.31	39.06	20
AAF-V	54	5.44	17.83	16.35	2.37	Yes	180.02	26.11	11

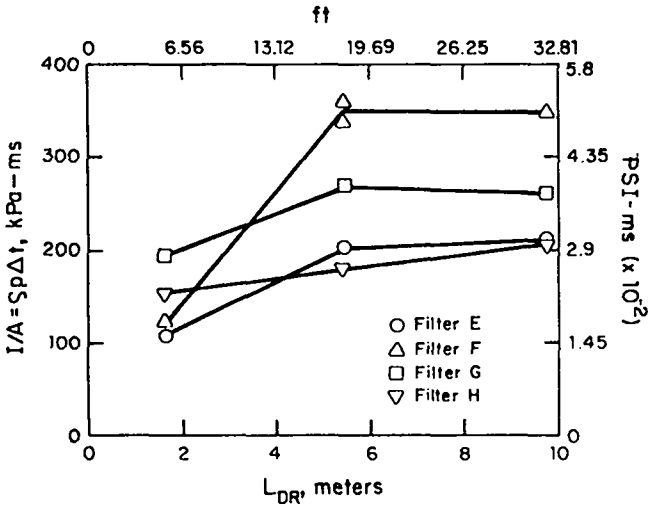

Fig. 17.
Shock impulse needed to just break HEPA filters after four additional tests at L_{DR} = 5.44 m.

A large amount of particulate was released through these points of failure (approximately 6.39 x 10^{15} particles). If the mean diameter, 0.46 μ, is used to calculate the volume of the particles, then about 325 cm^3 of particulate was released or 341.25 g (0.75 lb). This amounts to about one-third of the particulate orginally loaded on the filter.

Test number 59 was also of a Luwa V-type filter, but the shock over-pressure was reduced to 3.79 kPa (0.55 psi) to prevent filter failure. The amount of release was 1.9 x 10^{10} particles or 0.001 cm^3 of particulate. This corresponds to 1.05 mg by weight.

Finally, a loaded Flanders separatorless filter was subjected to a 3.86-kPa (0.56-psi) shock over-pressure for test number 62. In this case, 4.22 x 10^{10} particles were released amounting to 0.002 cm^3 or 2.1 mg of particulate.

D. Efficiency of Clean High-Capacity Filters

Section IV.D presents the results of subjecting a clean Luwa V-type filter to a shock over-pressure from air that had been seeded with polystyrene latex particulate. The shock over-pressure was 6.89 kPa (1.0 psi). Particulate challenging the filter during the test amounted to 4.59 x 10^{10} particles, whereas 1.32 x 10^{10} particles were counted downstream. Thus, the efficiency during the test was

$$\eta = \frac{4.59 \times 10^{10} - 1.32 \times 10^{10}}{4.59 \times 10^{10}} \times 100 = 71\% \quad .$$

Apparently, filter efficiency is reduced by a substantial amount from the nominal 99.97% for a shock over-pressure.

VI. APPLICATION OF RESULTS TO NUCLEAR SAFETY ANALYSIS

We believe that the results from this investigation will be useful to analysts concerned with the design and safety of nuclear facilities, particularly when high-capacity HEPA filters are being considered for installation. Typical safety analyses require predicting accident-induced pressure and flow surges throughout a nuclear facility ventilation system. These predicted values have limited use if the analyst does not know the structural limits or the response of critical components, such as HEPA filters, to these abnormal pressure transients. We have obtained supportive experimental data that, when coupled with predictive dynamic loadings, will allow the analyst to determine response of HEPA filters to simulated tornado and explosive loadings. In this section we will consolidate the results of the investigation into a form that will be directed toward safety analysts.

A. Structural Limits of High-Capacity HEPA Filters for Tornado Transients

The structural limits of high-capacity HEPA filters for simulated tornado loadings from four manufacturers are listed in Table IV.

The analyst needs to use the data from this table and also predict the tornado-induced pressures and flows at all filter locations using a method or a computer code similar to the TVENT code.[9] If any of the predicted peak pressures exceed the values listed in Table IV, the analyst should be concerned about possible filter failure and subsequent release to the atmosphere. If the analyst has no knowledge of the type of filter to be used in the facility, the upper structural limit to consider would be 11.2 kPa (1.6 psi) or perhaps even the lowest value of 9.0 kPa (1.3 psi).

B. Structural Limits of HEPA Filter for Explosive Transients

As can be seen from Table IV, the standard HEPA filters and the high-capacity HEPA filters respond differently to shock over-pressure. Clean HEPA filters of the standard type have a minimum-break over-pressure of about 2.0 psi (Table VI), and the high-capacity types have a minimum-break over-pressure of about 1.0 psi (Fig. 13.). Notice that the work of Anderson and Anderson gave a limiting pressure of 3.0 psi.[6] However, they did not mention the manufacturer of the filters they listed. Our tests show that the break pressure resulting from shock impingement is highly dependent on the manufacturer. Therefore, the safe shock over-pressure (that is, the shock over-pressure for which filter failure will not occur) should be taken to be less than 2.0 psi for standard HEPA filters and less than 1.0 psi for high-capacity HEPA filters. As in the

tornado-analysis case, a predictive method for explosively driven pressure waves throughout a ventilation system must be coupled with these results. The computer code EVENT developed at Los Alamos can serve as the predictive tool.[10]

From our studies of high-capacity HEPA filters, we found that shock impulse per unit area (I/A) was related to structural failure. The filters seem to have a property that causes them to fail at a particular value of I/A. If this value of I/A or greater is contained in an impinging shock pulse, the filters will fail during the shock over-pressure. The impulse present in any pressure wave can be calculated using the EVENT computer program. If there is not sufficient I/A contained within the shock pulse, then the filter may still fail because of the large magnitude of the airflow rate following the shock wave. Thus, the analyst must take great care when using I/A as a criterion. The safest approach would appear to be using the lowest I/A from Fig. 17 (that is, 100 kPa-ms) as the limiting I/A.

C. Structual Limits of Preloaded High-Capacity HEPA Filter for Explosive Transients

The results shown in Table III indicate that loaded high-capacity HEPA filters fail at a lower shock over-pressure than do clean filters. For example, the Luwa V-type failed at a pressure of 11.02 kPa (1.6 psi) when clean, but at 6.89 kPa (1.0 psi) when loaded (at a driver length of 5.44 m or 17.83 ft). Similarly, the Flanders separatorless filter failed at a shock over-pressure of 8.27 kPa (1.2 psi) when clean, but at about 5.99 kPa (0.87 psi) when loaded. Thus, the failure over-pressure appears to be reduced by about 40% for a Luwa V-type filter and by about 30% for a Flanders separatorless filter. An analyst should degrade the shock strength of filters that have been in use by at least 40%. Strengths of filters that have been subjected to acid environments or to intense radiation should obviously be further degraded, and these effects need investigation.

D. Material Loss From Loaded Filters

The guidance that can be offered to the safety analyst in this area is rather qualitative because of the limited number of tests. Our tests show that at the inital point of failure, large amounts of particulate can be released. Further, even if structural failure does not occur and the peak pressure is 50% below the failure point, significant amounts of particulate will be released. We suggest that the safety analyst consider filter efficiency as a criterion that will lower the pressure limit below 50% of the structural limit. Obviously, this area needs futher investigation.

E. Efficiency of High-Capacity Filters Subjected to Particulate Entrained Within the Shock Pulse

New generations of the EVENT computer code that predict explosive wave propagation also include a capability of simulating transport of material.[5] When this code's capabilities are coupled with the supportive experimental data developed in this section, better estimates of particulate release are possible. If the safety analyst uses the results from this study, he would allow 30% of the material to pass through the protective HEPA filter even if the impinging shock wave is below the filter's structural limit. However, the data in this area are very limited and should be used very carefully.

VII. SUMMARY AND CONCLUSIONS

This investigation involved determining the response of standard and high-capacity filters to simulated tornado and explosive transients. Most of the study was devoted to evaluating the effect of explosive transients, although several filters were subjected to simulated tornado transients. The effect of particulate loading on structural strength and filtration efficiency was also examined. We have included a section in the report with added detail on how the results may be used by those performing safety analyses of nuclear facilities. The conclusions reached in the investigation are outlined below.

A. Clean High-Capacity Filters Subjected to Simulated Tornado Transients

Clean high-capacity HEPA filters have lower structural limits for simulated tornado transients than standard HEPA filters.

B. Clean Standard and High-Capacity Filters Subjected to Simulated Explosive Transients

1. Standard HEPA filters fail at peak pressures significantly lower (13.78 kPa or 2.0 psi compared with 20.7 kPa or 3.0 psi) then the values reported in Ref. 5.
2. High-capacity HEPA filters fail at peak pressures significantly lower (6.89 kPa or 1.0 psi compared with 13.78 kPa or 2.0 psi) than those reported for standard filters in Ref. 1.
3. In general, the shock over-pressure needed to cause structural failure of HEPA filters increases as the shock-tube driver length decreases.
4. At short driver lengths, failure occurs after the shock impulse has passed through or has been absorbed by the filter. At long driver lengths, failure occurs during the shock impulse.

5. For short driver lengths, there is some evidence that the high residual flow rate of air behind the shock wave may cause filter failures rather than shock impulse. Further investigation of this point is needed because it has a significant effect on computer code predictions of ventilation system behavior during explosive transients.
6. A high probability exists that shock impulse needed to cause filter failure is constant for each type of filter at long driver lengths.
7. The filter manufacturer is a variable that has significant effect upon filter failure.

C. Preloaded Filters Subjected to Simulated Explosive Transients

High-capacity HEPA filters with preloaded particulate have structural limits that are 30 to 40% lower than clean filters. This result is not consistent with the results for standard HEPA filters reported in Ref. 1.

D. Material Release from Preloaded High-Capacity HEPA Filters

1. A large amount of particulate (as much as 340 g) can be released from a high-capacity filter when it is subjected to a shock impulse that only causes incipient structural failure.
2. When preloaded high-capacity filters are subjected to shock waves of approximately 50% of the structural limit, 1 to 2 mg of particulate is released.
3. The results in this area should be used carefully considering the limited test data available.

E. Efficiency of Clean High-Capacity Filters to Simulated Explosive Transients

1. The filter efficiency for explosive transients below structural failure can decrease by a substantial amount.
2. The results in this area should be used carefully considering the limited test data available.

ACKNOWLEDGMENTS

The authors gratefully acknowledge the efforts of H. Grothus, P. Ricketts, R. Lidh, C. Ricketts, J. Corkran, and K. Ziehl in operating the test facility and reducing data.

REFERENCES

1. W. S. Gregory, H. L. Horak, P. R. Smith, and C. I. Ricketts, "Structural Performance of HEPA Filters Under Simulated Tornado Conditions," Los Alamos National Laboratory report LA-9197-MS, NUREG/CR2565, submitted for publication.

2. W. S. Gregory and P. R. Smith, "Ventilation System Pressure Transients - Proposed Experiments and Shock Tube Conceptual Design," Los Alamos Scientific Laboratory report LA-7413-MS (September 1978).

3. D. LaPlante, P. R. Smith, and W. S. Gregory, "Ventilation System Pressure Transients - Small-Scale Shock Tube Results," Los Alamos Scientific Laboratory report LA-7726-MS (April 1979).

4. P. R. Smith and W. S. Gregory, "Investigation of Pressure Transients in Nuclear Filtration Systems - Construction Details of a Large Shock Tube," Los Alamos Scientific Laboratory report LA-8322-MS (April 1980).

5. R. W. Andrae, J. W. Bolstad, R. D. Foster, W. S. Gregory, H. L. Horak, E. S. Idar, R. A. Martin, P. K. Tang, C. I. Ricketts, and P. R. Smith, "Investigation of Air Cleaning System Response to Accident Conditions," Proc. 16th DOE Nuclear Air Cleaning Conference, 1980 (San Diego, California, 1980), pp. 1141-1164.

6. W. L. Anderson and T. Anderson, "Effects of Shock Overpressures on High Efficiency Filter Units," Proc. 9th AEC Air Cleaning Conference, CONF 660904, Vol. 1 (September 1966).

7. P. R. Smith, "Preliminary Shock Testing," New Mexico State University Engineering Experiment Station Final Report (July 1980).

8. A. J. Chapman and W. F. Walker, Introductory Gas Dynamics (Holt, Rinhart, and Winston, New York, 1971).

9. K. H. Duerre, R. W. Andrae, and W. S. Gregory, "TVENT - A Computer Program for Analysis of Tornado-Induced Transients in Ventilation Systems," Los Alamos Scientific Laboratory report LA-7397-M (July 1978).

10. P. K. Tang, R. W. Andrae, J. W. Bolstad, K. H. Duerre, and W. S. Gregory, "Analysis of Ventilation Systems Subjected to Explosive Transients--Far-Field Analysis," Los Alamos National Laboratory report LA-9094-MS (November 1981).

APPENDIX A

TABLE A-I

EXPECTED ERRORS IN S.I. UNITS

Filter Mnf	Test No.	Expected Errors $\int p\Delta t \pm$ error $\int p\Delta t$ kPa-ms	+ error kPa-ms	- error kPa-ms	
CAM	1	491.61	60.61	59.37	
MSA	3	377.29	60.61	59.37	
MSA	4	314.41	50.26	49.02	
AAF	6	583.87	60.61	59.37	
FLN	7	66.74	50.26	49.02	
FLN	8	166.17	45.58	44.47	
MSA	9	521.26	56.47	55.23	
CAM	10	609.52	54.40	53.16	
MSA	11	428.87	92.26	89.77	---Error is larger because no TM on film.
Luwa	12	405.43	58.54	57.30	
S.F.	14	222.01	48.20	46.95	
MSA	15	375.01	31.65	30.41	
FLN	17	229.6	25.44	24.20	
S.F.	21	222.71	33.72	32.48	
S.F.	22	262.01	26.89	20.06	
AAF-V	24	333.72	32.89	31.65	
AAF-V	25	206.85	26.89	20.06	
FLN_s	27	213.75	26.89	20.06	
AAF	30	317.86	53.57	52.33	
Luwa	32	136.52	1.38	2.07	
Luwa	33	120.66	2.07	2.07	
FLN_s	36	103.43	10.34	13.79	
FLN_s	37	107.56	2.07	2.07	
S.F.	41	192.37	9.65	41.37	---Error is larger because no TM on film.

APPENDIX A CONT

TABLE A-I CONT

EXPECTED ERRORS IN S.I. UNITS

Filter Mnf	Test No.	Expected Errors $\int p\Delta t \pm$ error $\int p\Delta t$ kPa-ms	+ error kPa-ms	- error kPa-ms
AAF-V	43	151.0	44.47	59.16
AAF	47	535.74	54.40	53.16
Luwa	48	345.44	30.20	28.96
Luwa	49	485.52	52.34	51.10
Luwa	50	335.10	37.85	36.61
Luwa	52	358.54	61.37	59.99
S.F.	53	268.91	69.43	68.40
AAF-V	54	179.75	82.88	81.84
FLN_s	55	204.57	46.47	45.44

Time: $\pm$ 3 ms

Pressure:		
	$\pm$ 0.207 kPa	tests 1--30
	$\pm$ 0.172 kPa	tests 31--37
	$\pm$ 0.103 kPa	tests 38--40, 44, 46
	$\pm$ 0.138 kPa	tests 41--43
	$\pm$ 0.041 kPa	test 45
	$\pm$ 0.124 kPa	tests 47, 49
	$\pm$ 0.110 kPa	test 48
	$\pm$ 0.090 kPa	tests 50--55

APPENDIX B

TABLE B-I

EXPECTED ERRORS IN ENGLISH UNITS

Filter Mnf	Test No.	Expected Errors $\int p\Delta t \pm$ error $\int p\Delta t$ psig-ms	+ error psig-ms	- error psig-ms	
CAM	1	71.3	8.79	8.61	
MSA	3	54.72	8.79	8.61	
MSA	4	45.6	7.29	7.11	
AAF	6	84.68	8.79	8.61	
FLN	7	9.68	7.29	7.11	
FLN	8	24.1	6.61	6.45	
MSA	9	75.6	8.19	8.01	
CAM	10	88.4	7.89	7.71	
MSA	11	62.2	13.38	13.02	---Error is larger because no TM on film.
Luwa	12	58.8	8.49	8.31	
S.F.	14	32.2	6.99	6.81	
MSA	15	54.4	4.59	4.41	
FLN	17	33.3	3.69	3.51	
S.F.	21	32.3	4.89	4.71	
S.F.	22	38.0	3.90	2.91	
AAF-V	24	48.4	4.77	4.59	
AAF-V	25	30.0	3.90	2.91	
FLN_s	27	31.0	3.90	2.91	
AAF	30	46.1	7.77	7.59	
Luwa	32	19.8	0.2	0.3	
Luwa	33	17.5	0.3	0.3	
FLN_s	36	15.0	1.5	2.0	
FLN_s	37	15.6	0.3	0.3	
S.F.	41	27.9	1.4	6.0	---Error is larger because no TM on film.

APPENDIX B CONT

TABLE B-I CONT

EXPECTED ERRORS IN ENGLISH UNITS

Filter Mnf	Test No.	Expected Errors $\int p\Delta t \pm$ error $\int p\Delta t$ psig-ms	+ error psig-ms	- error psig-ms
AAF-V	43	21.9	6.45	8.58
AAF	47	77.7	7.89	7.71
Luwa	48	50.1	4.38	4.2
Luwa	49	70.4	7.59	7.41
Luwa	50	48.6	5.49	5.31
Luwa	52	51.99	8.9	8.7
S.F.	53	38.99	10.1	9.9
AAF-V	54	26.06	12.0	11.9
FLN_s	55	29.66	6.7	6.6

Time: $\pm$ 3 ms

Pressure:	$\pm$ .03 psig	tests 1--30
	$\pm$ .025 psig	tests 31--37
	$\pm$ .015 psig	tests 38--40, 44, 46
	$\pm$ .02 psig	tests 41--43
	$\pm$ .006 psig	test 45
	$\pm$ .018 psig	tests 47, 49
	$\pm$ .016 psig	test 48
	$\pm$ .013 psig	tests 50--55

Printed in the United States of America
Available from
National Technical Information Service
US Department of Commerce
5285 Port Royal Road
Springfield, VA 22161
Microfiche $3.50 (A01)

Page Range	Domestic Price	NTIS Price Code	Page Range	Domestic Price	NTIS Price Code	Page Range	Domestic Price	NTIS Price Code	Page Range	Domestic Price	NTIS Price Code
001-025	$ 5.00	A02	151-175	$11.00	A08	301-325	$17.00	A14	451-475	$23.00	A20
026-050	6.00	A03	176-200	12.00	A09	326-350	18.00	A15	476-500	24.00	A21
051-075	7.00	A04	201-225	13.00	A10	351-375	19.00	A16	501-525	25.00	A22
076-100	8.00	A05	226-250	14.00	A11	376-400	20.00	A17	526-550	26.00	A23
101-125	9.00	A06	251-275	15.00	A12	401-425	21.00	A18	551-575	27.00	A24
126-150	10.00	A07	276-300	16.00	A13	426-450	22.00	A19	576-600	28.00	A25
									601-up	†	A99

† Add $1.00 for each additional 25 page increment or portion thereof from 601 pages up.

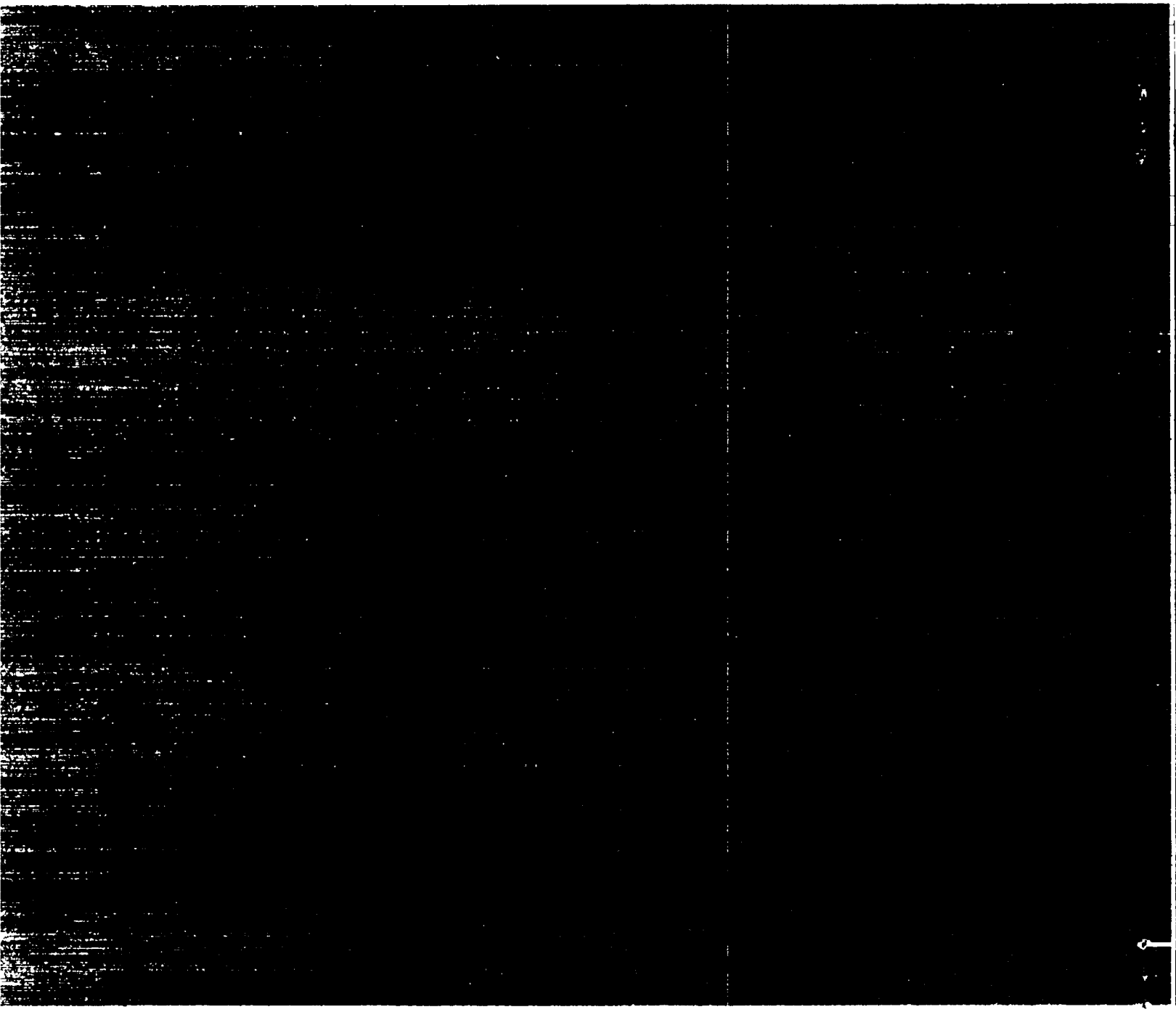

Los Alamos